# A Modified Light-Scattering Method for the Characterization of the Segmented Copolymer Poly(ethylene terephthalate-*co*-caprolactone)

**Chi Wu,\*,† Ka Fai Woo,† Xiaolie Luo,‡ and De-Zhu Ma‡**

*Department of Chemistry, The Chinese University of Hong Kong, Shatin, N.T., Hong Kong, and Department of Materials Science and Engineering, The University of Science & Technology of China, Hefei, Anhui, China*

ABSTRACT: The segmented copolymer poly(ethylene terephthalate-*co*-caprolactone (PET–PCL)) was successfully characterized by using a combination of static and dynamic laser light scattering (LLS). According to the Bushuk–Benoit light-scattering theory, at least *three solvents* with different refractive index increments have to be used to determine the weight-average molecular weight ($M_w$). Unfortunately, for samples with higher contents of PET (>50%), we were able to find only two such solvents. Thus, we were forced to adopt a modified LLS method wherein only *two solvents* were required. For each solvent, we first measured the apparent weight-average molecular weight ($M_{w,app}$) from static LLS. Then $M_{w,app}$ was used as a constraint to convert the line-width distribution from dynamic LLS into an apparent molecular weight distribution. Finally, after combining the two apparent molecular weight distributions, we determined not only the molecular weight distribution but also an estimate of the copolymer chain composition distribution. For samples with lower contents of PET, the $M_w$'s calculated from such obtained molecular weight distributions are comparable to those from the traditional three-solvent static LLS method.

## I. Introduction

The mechanical properties of the segmented copolymer poly(ethylene terephthalate-*co*-caprolactone (PET–PCL)) show that it is a thermal viscoelastic material. The hard PET segments can crystallize to form physical cross-linking points. Usually, the soft segments (PCL) are not expected to crystallize, and thus they contribute to the elasticity of the materials. As the amount of the hard segments increases, this segmented copolymer can gradually change from a low-modulus elastomer to a high-modulus tough plastic. Therefore, the characterization of this type of segmented copolymer, especially its molecular weight distribution and chain composition distribution, is crucially important to its various applications.

Laser light scattering (LLS), especially static or classic LLS, as an absolute analytical method has been well developed to characterize homopolymers in terms of the weight-average molecular weight ($M_w$), the z-average radius of gyration ($\langle R_g^2 \rangle_z^{1/2}$ or simply $R_g$), and the second virial coefficient ($A_2$) in various solvents and sometimes under extreme experimental conditions.[1–4] However, in contrast to the characterization of homopolymers, only a limited number of experimental results on copolymers have been reported. Among them, to our knowledge, only Chu et al.[5] have used dynamic LLS to characterize a copolymer which is actually a (quasi)terpolymer. The limited static LLS application to copolymers is partially due to the amount of work involved and partially due to the difficulty of finding at least three solvents with different refractive index increments ($\nu$). Dynamic LLS application to copolymers is mainly limited by the fact that polymer chains with different molecular weights and chain compositions can yield the same hydrodynamic radius, which is the same problem encountered in the application of size exclusion chromatography (SEC) to copolymers. Therefore, a few academic investigators have spent much time

in trying to develop LLS to the point where it could be used to characterize the molecular weight or determine the molecular weight distribution of a copolymer. However, the problem still remains to be solved. Nowadays, on the one hand, more and more applications of copolymers require that both the molecular weight and the chain composition distribution be known; on the other hand, dynamic LLS in the past 15 years has been developed into a standard technique in many academic and industrial polymer laboratories. It is our intention in this work to present a modified LLS method wherein a combination of static and dynamic LLS results will enable us to determine not only the weight-average molecular weight but also the molecular weight distribution and an estimate of the copolymer chain composition distribution.

It is well-known that the angular dependence of the excess absolute time-averaged scattered intensity (known as the excess Rayleigh ratio, $R_{vv}(\theta)$) of a polymer solution with a dilute concentration ($C$) and at a given scattering angle ($\theta$) can be expressed as[6]

$$\frac{KC}{R_{vv}(\theta)} \cong \frac{1}{M_w P(\theta)} + 2A_2 C \qquad (1)$$

where $K = 4\pi^2 n^2 \nu^2/(N_A \lambda_0^4)$, with $N_A$, $n$, $\lambda_0$, and $\nu$ being Avogadro's number, the solvent refractive index, the wavelength of light in vacuo, and the refractive index increment $dn/dC$, respectively. For a relatively short polymer chain, $P(\theta)$ can be related to $R_g$ by the approximation $1/P(\theta) \cong 1 + {}^1/_3 R_g^2 q^2$, where $q$, defined as $(4\pi n/\lambda_0) \sin(\theta/2)$, is the scattering vector. The accuracy of the measured $M_w$ is strongly dependent on $\nu$.

For a polydisperse copolymer with different molecular weight and chain composition distributions, $M_w$ determined by using eq 1 will be only an apparent weight-average molecular weight, $M_{w,app}$, which is defined as[7]

$$M_{w,app} = \int_0^\infty f_w(M) \left( \frac{\nu(M)}{\nu} \right)^2 M \, dM \qquad (2)$$

where $f_w(M)$ is the weight distribution and $\nu(M)$ is the refractive index increment for molecules with molecular

---

\* To whom correspondence should be addressed.
† The Chinese University of Hong Kong.
‡ The University of Science & Technology of China.

weight $M$ and weight distribution $f_w(M)$. We will denote $f_w(M)(\nu(M)/\nu)^2$ as the apparent weight distribution, $f_{w,\text{app}}(M)$. Based on the assumption of the additivity of $\nu$ for a segmented copolymer of A and B[8]

$$\nu(M) = w_A(M)\nu_A + w_B(M)\nu_B \qquad (3)$$

and

$$\nu = w_A\nu_A + w_B\nu_B \qquad (4)$$

where $w_A(M)$ and $w_B(M)$ [$\equiv 1 - w_A(M)$] are the weight fractions (chain composition) of A and B for a given polymer chain with fixed $M$ and $f_w(M)$, respectively, and $w_A$ and $w_B$ are the weight fractions (chain composition) for the overall copolymer. $w_A$ and $w_B$ are usually known parameters from polymerization. For a chosen solvent, $\nu_A$, $\nu_B$, and $\nu$ are constants for a given copolymer at fixed experimental conditions. It is obvious that for a uniform chain composition, i.e., $w_A(M) = w_A$, $w_B(M) = w_B$, and $\nu(M) = \nu$, we have $M_{w,\text{app}} = M_w$. It should be noted that eq 3 is not unique since different chain compositions can generate a polymer chain with identical $M$ and $f_w(M)$. As previously stated by Bushuk and Benoit,[7] eq 2 can be rewritten as

$$M_{w,\text{app}} = M_w + 2P(\Delta\nu/\nu) + Q(\Delta\nu/\nu)^2 \qquad (5)$$

with

$$\Delta\nu = \nu_A - \nu_B, \qquad M_w = \int_0^\infty f_w(M)M\,\mathrm{d}M$$

$$P = \int_0^\infty f_w(M)M[w_A(M) - w_A]\,\mathrm{d}M$$

$$Q = \int_0^\infty f_w(M)M[w_A(M) - w_A]^2\,\mathrm{d}M \qquad (6)$$

For each selected solvent, we are able to determine one pair of $M_{w,\text{app}}$ and $(\Delta\nu/\nu)$. According to eq 5, the minimum of *three solvents* are needed to determine $M_w$. It is known that $\nu$ can be related to the difference between the refractive index of a given polymer and solvent: namely, $\nu_A \sim (n_A - n_s)$, $\nu_B \sim (n_B - n_s)$, and $\Delta\nu \sim (n_A - n_B)$, where the dependence of $\Delta\nu$ on solvent is not as strong as that of $\nu_A$ or $\nu_B$. The choice of such three solvents must simultaneously satisfy the following conditions: first, the $\nu$ values of the three solvents should be as different as possible; second, the copolymer should be soluble in all of the chosen solvents; third, the final copolymer solutions at the incident laser wavelength should be as transparent as possible—i.e., the absorption should be as low as possible; and fourth, solution clarification, such as the removing of dust, should not be extremely difficult. In practice, the choice of such a set of three solvents for a given copolymer is very difficult or even impossible in some cases, such as for the PET–PCL samples with high PET contents (>50%). The difficulty is mainly due to visibility in light scattering or solubility.

## II. Theoretical Background

The details of dynamic LLS can be found elsewhere.[9] In dynamic LLS, a precise intensity–intensity time correlation function $G^{(2)}(t,\theta)$ in the self-beating mode can be measured, which has the following form:[9,10]

$$G^{(2)}(t,\theta) = \langle I(t,\theta)\,I(0,\theta)\rangle = A[1 + \beta|g^{(1)}(t,\theta)|^2] \qquad (7)$$

where $A$ is a measured baseline, $\beta$ is a parameter depending on the coherence of the detection, $t$ is the delay time, and $g^{(1)}(t,\theta)$ is the normalized first-order electric field time correlation function. For a polydisperse sample, $g^{(1)}(t,\theta)$ is related to the line-width distribution $G(\Gamma)$ by

$$g^{(1)}(t,\theta) = \langle E(t,\theta)\,E^*(0,\theta)\rangle = \int_0^\infty G(\Gamma)\mathrm{e}^{-\Gamma t}\,\mathrm{d}\Gamma \qquad (8)$$

where the line-width $\Gamma$ usually depends on both $C$ and $\theta$. This dependence can be expressed as[11]

$$\frac{\Gamma}{q^2} = D(1 + k_d C)(1 + fR_g^2 q^2) \qquad (9)$$

where $D$ is the translational diffusion coefficient at $C = 0$ and $q = 0$, $f$ is a dimensionless number, and $k_d$ is the diffusion second virial coefficient. The value of $f$ depends on the chain structure, polydispersity, and solvent quality. For polymers with flexible chains in a good solvent, $f$ is between 0.1 and 0.2.[11] Both thermodynamic and hydrodynamic interactions contribute to $k_d$, which can be further expressed as[12]

$$k_d = 2A_2 M_w - C_D N_A R_h^3/M_w \qquad (10)$$

where $C_D$ is an empirical positive constant and $R_h$ is the hydrodynamic radius. On the basis of eq 9, for a given set of $f$ and $k_d$, $G(\Gamma)$ is readily transferred into $G(D)$.

After combining eqs 1, 2, and 8 at the conditions of $C \to 0$, $\theta \to 0$, and $t \to 0$, we have

$$R_{vv}(\theta) = KC\int_0^\infty f_w(M)M\left(\frac{\nu(M)}{\nu}\right)^2\mathrm{d}M \sim \langle I\rangle \qquad (11)$$

and

$$g^{(1)}(0,\theta) = \langle E(0,\theta)\,E^*(0,\theta)\rangle = \int_0^\infty G(\Gamma)\,\mathrm{d}\Gamma \sim \langle I\rangle \qquad (12)$$

which lead to

$$\int_0^\infty G(D)\,\mathrm{d}D = \gamma\int_0^\infty f_w(M)M\left(\frac{\nu(M)}{\nu}\right)^2\mathrm{d}M \qquad (13)$$

where $\gamma$ is a normalization constant. Normally, $D$ can be related to $M$ by using two scaling constants, $k_D$ and $\alpha_D$, i.e.

$$D = k_D M^{-\alpha_D} \qquad (14)$$

where both $k_D$ and $\alpha_D$ are independent of $M$ for a given solvent and chain composition for a given set of experimental conditions. By using eq 14, we can rewrite eq 13 as

$$\int_0^\infty G(D)\frac{\mathrm{d}D}{\mathrm{d}M}\,\mathrm{d}M = \gamma\int_0^\infty f_w(M)M\left(\frac{\nu(M)}{\nu}\right)^2\mathrm{d}M \qquad (15)$$

After comparing both sides of eq 15, we have

$$f_{w,\text{app}}(M) = f_w(M)\left(\frac{\nu(M)}{\nu}\right)^2 \propto \frac{G(D)}{M}\frac{\mathrm{d}D}{\mathrm{d}M} \qquad (16)$$

where all proportionality constants have been omitted since they are irrelevant to both distributions. For a given set of $k_D$ and $\alpha_D$, we are able to convert $G(D)$ into $f_{w,\text{app}}(M)$ by using eqs 14 and 16.

As stated by Chu et al.,[5] if we repeat the above procedure by using two solvents (denoted s1 and s2) with different $\nu(M)$ and $\nu$, even for a given copolymer sample, we will have two different apparent weight distributions, $f_{w,\text{app,s1}}$-

$(M) = f_w(M)(\nu(M)/\nu)_{s1}^2$ and $f_{w,app,s2}(M) = f_w(M)(\nu(M)/\nu)_{s2}^2$. By using eq 3, we find that the ratio of the two apparent weight distributions is

$$\frac{f_{w,app,s1}(M)}{f_{w,app,s2}(M)} = \left\{ \frac{\nu_{s2}}{\nu_{s1}} \frac{w_A(M)\nu_{A,s1} + [1 - w_A(M)]\nu_{B,s1}}{w_A(M)\nu_{A,s2} + [1 - w_A(M)]\nu_{B,s2}} \right\}^2 \quad (17)$$

where $\nu_{s1}$, $\nu_{s2}$, $\nu_{A,s1}$, $\nu_{A,s2}$, $\nu_{B,s1}$, and $\nu_{B,s2}$ can be determined by using a differential refractometer. Equation 17 shows that $w_A(M)$, the chain composition distribution, can be calculated from two apparent weight distributions if the values of $\nu_{s1}$, $\nu_{s2}$, $\nu_{A,s1}$, $\nu_{A,s2}$, $\nu_{B,s1}$, and $\nu_{B,s2}$ are known. After obtaining $w_A(M)$, we are ready to calculate first $\nu(M)$, then $f_w(M)$, and finally $M_w$.

## III. Experimental Section

**Samples.** The synthesis of segmented copolymers of poly-(ethylene terephthalate-*co*-caprolactone) (PET-PCL) with different amounts of PET was performed in two separate steps.[13] The first involves the esterification of terephthalic acid and ethylene glycol with a catalyst at 190 °C; the second is a catalyzed polycondensation of poly(caprolactone) ($M_n = 2000$) with ethylene terephthalate under vacuum at 250 °C. The PET content in the two samples used in the present work is 13% and 58% by weight, respectively. They are denoted 13% PET-PCL and 58% PET-PCL hereafter. The samples were further fractionated by using a precipitation method where chloroform and methanol were used as solvent and precipitator, respectively. Two fractions with different weight-average molecular weights, but a similar composition, were obtained.

**Solution Preparation.** Four analytical grade organic solvents (butanone, ethyl acetate, tetrahydrofuran, and chloroform) were used without further purification. The concentration was in the range $4 \times 10^{-4}$ to $8 \times 10^{-3}$ g/mL. All solutions were clarified at room temperature by using a 0.22 $\mu$m Millipore filter to remove dust.

**Refractive Index Increment.** All refractive index increments were determined by using a novel differential refractometer,[14] which is incorporated into our LLS spectrometer where the same laser light source is used in both LLS and the refractometer. Therefore, the obtained refractive index increments will not require wavelength correction. In addition, a 6-mm position-sensitive detector (Hamamatsu) and a 16 bit analog-to-digital data acquisition card (National Instrument) were used to detect the laser beam shift caused by the refractive index difference between the polymer solution and the solvent, which not only increases the accuracy of the measured $\nu$ but also makes a large amount of $\nu$ measurements possible and easier.

**Laser Light Scattering.** A commercial laser light scattering spectrometer (ALV DLS/SLS-5000, Langen in Hessen, Germany) was used with an argon ion laser (Coherent INNOVA 90, operated at a wavelength of 488 nm and 400 mW) as the light source. The primary beam is vertically polarized. A compensated beam attenuator (Newport M-925B) was used to regulate the incident laser light intensity to avoid possible localized heating in the light-scattering cuvette. The intensity–intensity time correlation functions were measured by an ALV 5000 multiple-$\tau$ digital correlator. The correlation functions were accumulated until the net photon count was beyond $10^6$ per second. We insisted that the difference between the measured and calculated baselines be no more than 0.1%. The instrumental details can be found elsewhere.[10] All LLS was done at 25.0 $\pm$ 0.1 °C.

## IV. Results and Discussion

Table 1 shows the $\nu$ values of the PET–PCL copolymers together with the $\nu$ values of both PCL and PET homopolymers in different solvents. The experimental details of how to measure and obtain these $\nu$ values can be found elsewhere.[14,15] It should be stated that the $\nu$ values of the lower and higher molecular weight fractions are very similar, which implies that their chain composition distributions are very similar and the fractionation is

**Table 1. Specific Refractive Index Increments ($\nu$) of Segmented PET–PCL Copolymers Together with PET and PCL Homopolymers in Different Solvents at 25 °C[a]**

| sample | $\nu$ (mL/g) | | | |
|---|---|---|---|---|
| | chloroform | THF | ethyl acetate | butanone |
| 13% PET-PCL | 0.071 | 0.090 | 0.122 | 0.120 |
| 58% PET-PCL | 0.105 | 0.129 | | |
| PCL homopolymer | 0.060 | 0.079 | 0.110 | 0.108 |
| PET homopolymer | 0.143 | 0.165 | 0.200 | 0.194 |

[a] The relative uncertainty of all measured $\nu$ is about $\pm$1%.
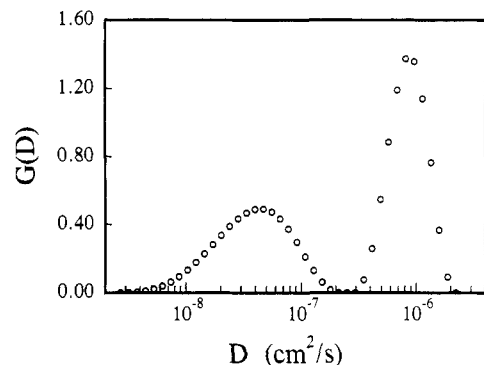


**Figure 1.** Typical diffusion coefficient distribution of the 58% PET–PCL sample in ethyl acetate at 25 °C.
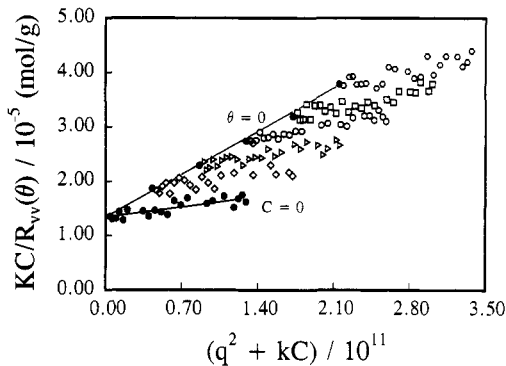


**Figure 2.** Typical static Zimm plot of the 13% PET–PCL sample in chloroform at 25 °C, where five concentrations range from $7.90 \times 10^{-4}$ to $3.95 \times 10^{-3}$ g/mL.

mainly based on the molecular weight, not on the composition. We will come back to this point later. The 58% PET–PCL sample is insoluble in butanone and partially soluble in ethyl acetate due to the high content of PET segments. Figure 1 shows a typical diffusion coefficient distribution of the 58% PET–PCL sample in ethyl acetate at 25 °C. The peak located at higher $D$ corresponds to dissolved individual PET–PCL molecules, but the peak at lower $D$ shows aggregated or undissolved PET–PCL molecules. Since $G(D)$ is proportional to the scattered laser light intensity, i.e., $G(D) \propto f_n(M)M^2$, where $f_n(M)$ is the number distribution,[16] dynamic LLS is a very sensitive tool to detect the larger aggregates. It should be pointed out that the number of PET–PCL aggregates in solution is very small, even though the area under the peak corresponding to the aggregates is large in $G(D)$ vs $D$. This is why these possible aggregates were overlooked in the past in other types of experimental methods, such as in viscometry or even in static LLS,[17] where both butanone and ethyl acetate were used as solvents without notice of the aggregates.

Figure 2 shows a typical static Zimm plot which incorporates $\theta$ and $C$ extrapolations on a single grid for the 13% PET–PCL sample in chloroform at 25 °C. On the basis of eq 1, we were able to calculate $M_{w,app}$, $A_{2,app}$,

**Table 2. Summary of Laser Light Scattering Results of Three Segmented PET–PCL Copolymers in Different Solvents at 25 °C**

| sample | solvent | $10^{-4}M_w$, app | $10^3A_2$, app/(mol·mL/g$^2$) | $R_g$, app/nm | $10^7\bar{D}/$(cm$^2$/s) | $\bar{k}_d/$(mL/g) | $\bar{f}$ |
|---|---|---|---|---|---|---|---|
| 13% PET–PCL | chloroform | 7.84 | 2.4 | 28 | 4.30 | ~10 | ~0.1 |
| low $M$ | THF | 7.35 | 1.2 | 22 | 5.43 | ~20 | ~0.1 |
| 13% PET–PCL | chloroform | 27.9 | 1.2 | 30 | 2.33 | ~90 | ~0.1 |
| high $M$ | THF | 29.6 | 0.8 | 28 | 3.11 | ~80 | ~0.1 |
| 58% PET–PCL | chloroform | 3.27 | 2.4 | ~10$^a$ | 6.37 | ~20 | ~0.1 |
| | THF | 3.53 | 1.1 | ~10$^a$ | 7.43 | ~10 | ~0.1 |

$^a$ This small $R_{g,app}$ was an estimated value.
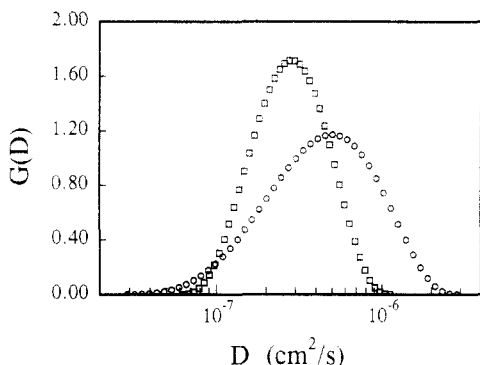


**Figure 3.** Diffusion coefficient distributions of the low-$M$ (O) and high-M (□) 13% PET–PCL samples in tetrahydrofuran at 25 °C.

and $R_{g,app}$ from the extrapolation of $[KC/R_{vv}(\theta)]_{\theta\to0,C\to0}$, $[KC/R_{vv}(\theta)]_{\theta\to0}$ vs $C$, and $[KC/R_{vv}(\theta)]_{C\to0}$ vs $q^2$, respectively. The results are summarized in Table 2. We should realize that the error associated with $R_g$ is more than 20% because the size of the PET–PCL copolymers is very small. The positive values of $A_{2,app}$ show that for the 13% PET–PCL sample all four solvents are good solvents at 25 °C. However, the less positive $A_{2,app}$ shows that as solvents both ethyl acetate and butanone are not as good as either chloroform or tetrahydrofuran. The values of $M_{w,app}$ are different from each other in two chosen solvents. In chloroform, the value of $R_{g,app}$ for the low-$M$ 13% PET–PCL sample is very similar to that of polystyrene with a similar chain length in good solvent, which shows that the segmented copolymer chain is still very flexible, even though it contains the PET segments. This flexibility is mainly due to the flexible ether linkages in the main copolymer chain.

On the basis of eq 9, we can respectively calculate the apparent $D$, $k_d$, and $f$ from $(\Gamma/q^2)_{\theta\to0,C\to0}$, $(\Gamma/q^2)_{\theta\to0}$ vs $C$, and $(\Gamma/q^2)_{C\to0}$ vs $q^2$. Experimentally, we found that $\bar{\Gamma}/q^2$, where $\bar{\Gamma} = \int_0^\infty G(\Gamma)\Gamma\,d\Gamma$, is nearly independent of $q^2$, which leads to a small value of $f \sim 0.1$, and the dependence of $\bar{\Gamma}/q^2$ on $C$ is less than that of $KC/R_{vv}(\theta)$ on $C$, which is reasonable since $k_d$ in eq 10 contains one negative term in comparison with the only term of $2A_2M_w$ in static LLS. The extrapolation results of the average $\bar{D}$, $\bar{k}_d$, and $\bar{f}$ for both the 13% and 58% PET–PCL samples are also listed in Table 2. The small $\bar{k}_d$ and $\bar{f}$ values show that the correction of a measured $\Gamma/q^2$ to $D$ is at most a few percent.

Figure 3 shows typical diffusion coefficient distributions of the low-$M$ and high-$M$ 13% PET–PCL samples in tetrahydrofuran at 25 °C. On the basis of eq 16, to convert $G(D)$ into $f_{w,app}(M)$, we have to find d$D$/d$M$, i.e., both $k_D$ and $\alpha_D$. In previous papers,[18–20] we have shown that $M_w$ (here, it should be $M_{w,app}$) can be calculated from $G(D)$ by

$$(M_w)_{calcd} = \frac{k_D^{1/\alpha_D}\int_0^\infty G(D)\,dD}{\int_0^\infty G(D)D^{1/\alpha_D}\,dD} \quad (18)$$

**Table 3. List of the Calculated Values of $k_D$ and $\alpha_D$ at 25 °C and Summary of $M_w$ and $M_w/M_n$ from Figure 6**

| sample | solvent | $k_D$ | $\alpha_D$ | $M_w$ | $M_w/M_n$ |
|---|---|---|---|---|---|
| 13% PET–PCL | chloroform | $5.3\times10^{-4}$ | 0.59 | $6.7\times10^4$ | 1.9 |
| | THF | $6.0\times10^{-4}$ | 0.58 | | |
| 58% PET–PCL | chloroform | $5.5\times10^{-4}$ | 0.62 | $3.4\times10^4$ | 1.8 |
| | THF | $5.8\times10^{-4}$ | 0.60 | | |

For two samples with similar composition but different average molecular weights, we have two measured $M_{w,app}$ values from static LLS and two calculated $G(D)$ values from dynamic LLS, denoted as $M_{w,app,1}$, $M_{w,app,2}$, $G_1(D)$, and $G_2(D)$. We also have two $(M_{w,app})_{calcd}$ values based on eq 18, denoted as $(M_{w,1})_{calcd}$ and $(M_{w,2})_{calcd}$. The ratio of $(M_{w,1})_{calcd}$ and $(M_{w,2})_{calcd}$ is

$$\frac{(M_{w,1})_{calcd}}{(M_{w,2})_{calcd}} = \frac{[\int_0^\infty G_1(D)\,dD][\int_0^\infty G_2(D)D^{1/\alpha_D}\,dD]}{[\int_0^\infty G_2(D)\,dD][\int_0^\infty G_1(D)D^{1/\alpha_D}\,dD]} \quad (19)$$

Each calculated $(M_{w,app})_{calcd}$ should equal the corresponding measured $M_{w,app}$, which means that the left side of eq 19 can be replaced by the ratio $M_{w,app,1}/M_{w,app,2}$. Thus, there is only one unknown parameter $\alpha_D$ in eq 19. After iterating $\alpha_D$, we are able to find a proper $\alpha_D$ which minimizes the difference between both sides of eq 19. With this $\alpha_D$, we can further determine the value of $k_D$ from $M_{w,app}$ and $G(D)$ by using eq 18. The values of $k_D$ and $\alpha_D$ for both the 13% and 58% PET–PCL samples in tetrahydrofuran and chloroform are summarized in Table 3. The values of $\alpha_D$ show that both chloroform and tetrahydrofuran are good solvents for the PET–PCL samples. For the 58% PET–PCL sample, $\alpha_D$ is slightly larger than the maximum value of 0.6 predicted for a flexible linear polymer chain in a good solvent. This suggested that the copolymer chain in the 58% PET–PCL sample is slightly extended, which is reasonable because there exists a large amount of PET hard segments in the sample. Having $k_D$ and $\alpha_D$, we are ready to transfer $G(D)$ in Figure 3 into $f_{w,app}(M)$ on the basis of eq 16.

Figure 4 shows two apparent weight distributions based on the two diffusion coefficient distributions in Figure 3 for the low-$M$ (O) and high-$M$ (□) 13% PET–PCL samples. After repeating the above static and dynamic LLS measurements in chloroform, we were able to obtain another set of apparent weight distributions for each PET–PCL sample. According to eq 17, by using the values of $\nu$ in both tetrahydrofuran and chloroform in Table 1 and the ratio of $f_{w,app,CHCl_3}(M)$ to $f_{w,app,THF}(M)$, we were able to calculate $w_{PET}(M)$ as a function of $M$.

Figure 5 shows calculated chain composition distributions for the low-$M$ (O) and high-$M$ (□) 13% PET–PCL samples. It shows that the PET content increases with $M$ when $M < \sim4\times10^4$ and approaches a constant value of $\sim14\%$ in the high molecular weight range. For the 58% PET–PCL sample, the composition distribution is nearly a constant. The composition distribution of the high-$M$
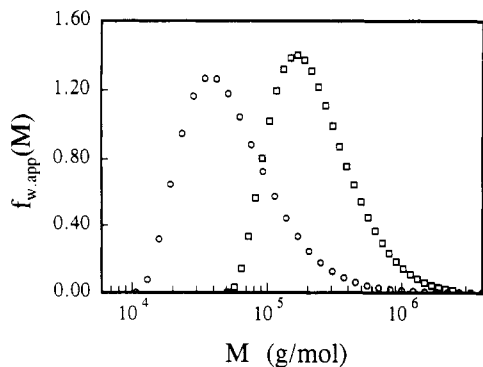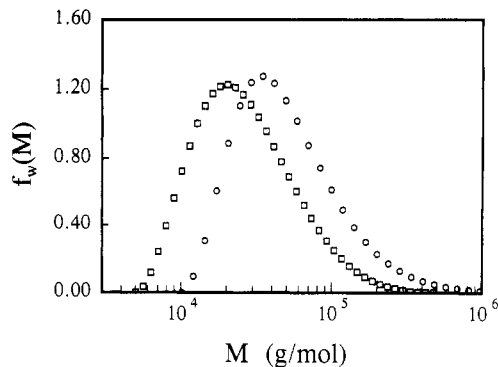
**Figure 4.** Apparent weight distributions of the low-$M$ (O) and high-$M$ (□) 13% PET–PCL samples in tetrahydrofuran, which were calculated from the distributions in Figure 3.
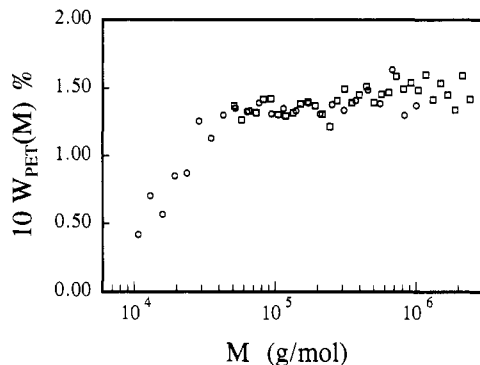


**Figure 5.** Calculated composition distributions of the low-$M$ (O) and high-$M$ (□) 13% PET–PCL samples.

13% PET–PCL sample overlaps with that of the low-$M$ 13% PET–PCL sample in the same molecular weight range, which indirectly indicates that the estimation of the composition distribution is reasonable. The lower content of PET in the low molecular weight range might be explained by the synthetic procedure. As mentioned before, the synthesis is a two-step process. First, the PET segments were made by a polycondensation, and then the PCL segments ($M_n$ = 2000) were added for further polycondensation. It should be noted that in the second stage, the average molecular weight of the PET segments should be higher than that of the initial PCL segments, and for the 13% PET–PCL sample, there was an excess of PCL segments in the reaction vessel. Therefore, it is reasonable to assume that the low molecular weight portion of the 13% PET–PCL sample will be richer in PCL segments or, equivalently, will contain fewer PET segments. Having $w_{PET}(M)$, we can first calculate $\nu(M)$ on the basis of eq 3 and then the true weight distribution $f_w(M)$ from $f_{w,app}(M)$ according to the definition of $f_{w,app}(M)$.

Figure 6 shows weight distributions for the 13% PET–PCL sample (□) and the 58% PET–PCL sample (O). From these distributions, we calculated $M_w$ and the polydispersity index $M_w/M_n$, which are also listed in Table 3. Since the low-$M$ 13% PET–PCL sample dissolves in all four solvents listed in Table 1, we were able to calculate its $M_w$ only from its static LLS results by using the traditional three-solvent method. Figure 7 shows an associated Benoit plot of $M_{w,app}$ versus $\Delta\nu/\nu$, where the circles are the experimental results and the dashed line is a least-squares fitting of $M_{w,app}$ = 6.60 × 10⁴ – 4.10 × 10³·($\Delta\nu/\nu$) + 1.25 × 10⁵($\Delta\nu/\nu$)². Therefore, on the basis of eq 5, $M_w$ = 6.60 × 10⁴, which is very close to the listed value of $M_w$ obtained by using only two solvents. This leads us to believe that the calculated $M_w$ for the 58% PET–PCL sample should be close to the true weight-average mo-



**Figure 6.** Calculated molecular weight distributions of the 13% PET–PCL sample (O) and the 58% PET–PCL sample (□).
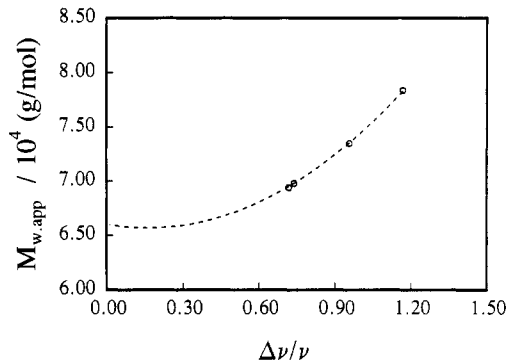


**Figure 7.** Benoit plot of $M_{w,app}$ versus $\Delta\nu/\nu$, where the circles are the experimental results and the dashed line is a least-squares fitting of $M_{w,app}$ = 6.60 × 10⁴ – 4.10 × 10³($\Delta\nu/\nu$) + 1.25 × 10⁵·($\Delta\nu/\nu$)².

lecular weight. For both the 13% and 58% PET–PCL samples, the respective polydispersity index values of 1.9 and 1.8 in Table 3 are very reasonable in comparison with the prediction of $M_w/M_n$ ≤ 2.0 for a polycondensation reaction.

## V. Conclusion

By adopting a modified laser light scattering method, i.e., a combination of static and dynamic light scattering results, we could readily characterize a segmented copolymer by using only *two solvents* instead of *three solvents* as required in the Bushuk–Benoit method. This modified method not only provides us with an alternative data analysis procedure but also enables us to characterize some special copolymers, e.g., the 58% PET–PCL sample in the present work, for which three appropriate solvents cannot be found. By using this *two-solvent* method, we can obtain both the molecular weight and chain composition distributions. It should be emphasized that due to the experimental uncertainties and errors associated with all calculations, especially with the Laplace inversion of the measured intensity–intensity time correlation function, the calculated composition is only an estimate.

## References and Notes

(1) Ying, Q.; Chu, B.; Qian, R. *Polymer* **1985**, *26*, 1408.
(2) Chu, B.; Wu, C. *Macromolecules* **1986**, *19*, 1285.
(3) Chu, B.; Wu, C.; Buck, W. *Macromolecules* **1988**, *21*, 397.

(4) Wu, C.; Zuo, J.; Chu, B. *Macromolecules* **1989**, *22* (2), 838.

(5) Chu, B.; Ying, Q.; Lee, D. C.; Wu, D. Q. *Macromolecules* **1985**, *18*, 1962.

(6) Debye, P. *J. Phys. Colloid Chem.* **1947**, *51*, 18.

(7) Bushuk, W.; Benoit, H. *Can. J. Chem.* **1958**, *36*, 1616.

(8) Stockmayer, W. H.; Moore, L. D., Jr.; Fixman, M.; Epstein, B. N. *J. Polym. Sci.* **1955**, *16*, 517.

(9) Pecora, R. *Dynamic Light Scattering*; Plenum Press: New York, 1976.

(10) Chu, B. *Laser Light Scattering*; Academic Press: New York, 1974.

(11) Stockmayer, W. H.; Schmidt, M. *Pure Appl. Chem.* **1982**, *54*, 407; *Macromolecules* **1984**, *17*, 509.

(12) Yamakawa, H. *Modern Theory of Polymer Solutions*; Harper and Row: New York, 1971.

(13) Lau, X.; Ma, D. Z.; Du, D. Z. *J. Univ. Sci. Technol. China* **1986**, *16* (3), 280.

(14) Wu, C.; Xia, K.-Q. *Rev. Sci. Instrum.* **1994**, *65*, 587.

(15) Wu, C.; Ma, D. Z.; Luo, X. L.; Chan, K. K.; Woo, K. F.; So, K. L. *J. Appl. Polym. Sci.*, in press.

(16) Wu, C. *Macromolecules* **1993**, *26*, 3821.

(17) Chu, Z.; Ma, D. Z.; Luo, X. L. *Chinese J. Appl. Chem.* **1986**, *3* (1), 57.

(18) Wu, C.; Lilge, D. *J. Appl. Polym. Sci.* **1993**, *50*, 1753.

(19) Wu, C. *Macromolecules* **1993**, *26*, 3821.

(20) Wu, C. *Macromolecules* **1993**, *26*, 5423.